

KINEMATIC ANALYSIS AND DESIGN OF A COMPLIANT MICROPLATFORM

Julio Correa¹, Carl Crane², Huikai Xie²

¹Universidad Pontificia Bolivariana, Medellín, Colombia

²University of Florida: P.O. Box 116300, Gainesville, FL, 32611

Mechanisms formed by rigid links and rigid joints are well suited to work at the macro-scaled world. However when the dimensions of the systems are on the order of microns, limitations due to manufacturing processes impose severe limitations, and the generation of motion requires alternative approaches.

Most devices for micro-electro-mechanical systems (MEMS) are basically planar devices. This is due the current manufacturing techniques that are derived from the IC industry. Thus, creating 3D structures at the micro level is a difficult task. This paper presents a new approach for a spatial microplatform that incorporates compliant elements in order to allow for a desired range of spatial motion without the need for complicated mechanical or stress concentrated joints. It has application to micro-assembly tasks where the platform can be used as a 'finger tip' to manipulate micro-scaled components.

I. INTRODUCTION

Out of plane actuators can convert input signals into displacements normal to the surface of a substrate. Three-dimensional microdevices are useful for different tasks as for example, object positioning, micromanipulators, optical scanners, tomographic imaging, optical switches, microrelays, adjustable lenses and bio-MEMS applications. References by Chen¹, Fu², Jain³, Ebefors⁴, Suh⁵, Schweizer⁶, Jensen⁷, and Bamberger⁸ provide an overview of some of recent advancements.

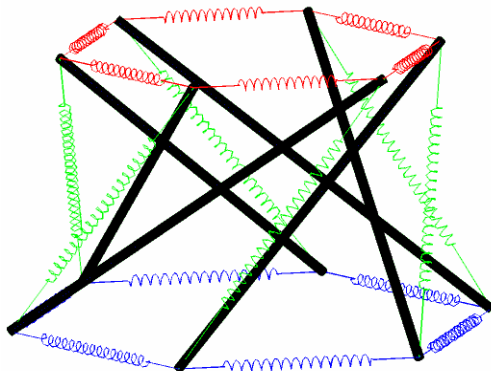


Fig. 1. Tensegrity Structure

The approach utilized here to achieve a spatial device incorporates the principles of tensegrity. The word tensegrity is a contraction of tension and integrity and refers to structures formed by rigid and elastic elements that maintain their shape due only to their configuration. Rigid elements do not touch one another and they do not require external forces to maintain their unloaded position. Fig. 1 shows a prismatic tensegrity structure where the elastic elements are represented by springs.

Tensegrity structures were discovered by architects in the middle of the last century. Research began with Fuller⁹. First contributions were made by Kenner¹⁰ and Calladine¹¹. Static and dynamic analysis studies have been made by Murakami¹² and Crane et al¹³. Proposed applications include antennas (Knight¹⁴), flight simulators (Sultan and Corless¹⁵), deployable structures (Tibert and Pellegrino¹⁶), and force and torque sensors (Sultan and Skelton¹⁷). Tensegrity has been also proposed by Ingber¹⁸ to explain the deformability of cells.

Due to the presence of elastic ties, tensegrity structures are foldable. If in the folded position external constraints are released, they can recover suddenly their original shape by themselves. The deployment can be also achieved in a controlled way using telescopic struts or controlling the elastic ties.

II. DESCRIPTION OF DEVICE

Fig. 2 depicts the device that is addressed in this research. It can be considered as a simplification of the tensegrity system presented in Fig. 1. The system maintains its shape due to the upward deflections of the beams. It is formed by three sets of bimorph actuators which transmit their motion to the central platform through compliant joints. The position of the device is influenced by the stiffness and free lengths of the ties, the location and nature of the joints, and the length and the current curvature of the beams.

III. KINEMATIC FORWARD ANALYSIS

A kinematic forward analysis has been completed for this design. In this analysis it is assumed that the three

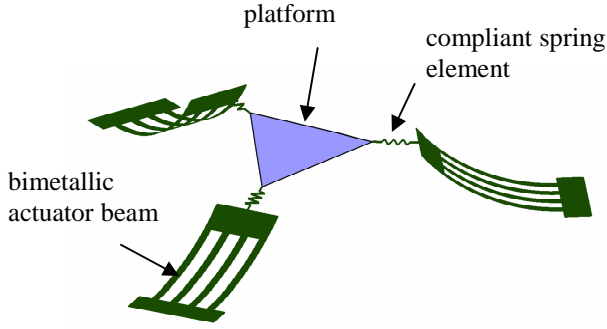


Fig 2. Compliant Microplatform

spring constants and spring free lengths are known together with the dimensions of the moving platform and the location of the base points of the actuator beams. It is also assumed that the platform is massless and that the deflections of the actuator beams due to the forces of the spring element are negligible. This last assumption has been verified via strength of materials calculations.

Fig. 3 depicts the device in a general position. In the forward analysis the location of points Q_i with respect to a global reference system are given and the objective is to evaluate the coordinates of points P_i with respect to the global system A.

The solution can be performed using a Newtonian approach or an energy approach. The Newtonian approach is preferred here because it gives a better understanding of the geometry of the system.

Since the platform is massless, the external forces acting on the platform are due only to the three springs. Equilibrium of forces yields

$$f_1 \underline{s}_1 + f_2 \underline{s}_2 + f_3 \underline{s}_3 = \underline{0} \quad (1)$$

where \underline{s}_i is the unit vector from P_i to Q_i and f_i is the magnitude of the force in each spring.

Since the springs are linear, each force magnitude in Equation 1 can be expressed as a function of its stiffness and its deformation as follows

$$k(d_1 - d_0) \underline{s}_1 + k(d_2 - d_0) \underline{s}_2 + k(d_3 - d_0) \underline{s}_3 = \underline{0} \quad (2)$$

where d_i is the actual length and d_0 is the free length of spring i .

When the platform is working, the current lengths are always greater than the free lengths, and then the coefficients in Equation 2 are different from zero. It is clear that vectors \underline{s}_1 , \underline{s}_2 , and \underline{s}_3 are linearly dependent. From Brand¹, a necessary and sufficient condition that three vectors be linearly dependent is that they be coplanar. From the definition of \underline{s}_i , this result implies that despite the spatial motion of the platform, points Q_1 , Q_2 ,

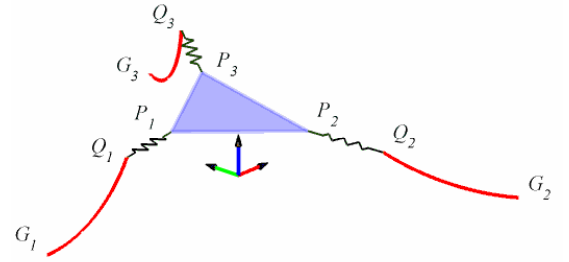


Fig 3. Device in General Position

Q_3 , P_1 , P_2 , and P_3 lie in the same plane and Equation 1 can be written as

$$f_1 \begin{bmatrix} s_{1x} \\ s_{1y} \end{bmatrix} + f_2 \begin{bmatrix} s_{2x} \\ s_{2y} \end{bmatrix} + f_3 \begin{bmatrix} s_{3x} \\ s_{3y} \end{bmatrix} = \underline{0} \quad (3)$$

where s_{ix} and s_{iy} are the rectangular components of the unit vector \underline{s}_i expressed in terms of a coordinate system whose z axis is normal to the plane of the moving platform.

The moment of the force $f \underline{s}$ with respect to an arbitrary point V is a vector perpendicular to the plane of the forces with magnitude $f * p$, where p is the perpendicular distance between V and the line of action of force $f \underline{s}$. Equilibrium of forces establishes that the summation of moments with respect to the arbitrary point V must be zero and thus

$$f_1 p_1 + f_2 p_2 + f_3 p_3 = 0 \quad (4)$$

Equation 3 can be combined with Equation 4 to obtain, see Duffy²

$$\begin{bmatrix} s_{1x} & s_{2x} & s_{3x} \\ s_{1y} & s_{2y} & s_{3y} \\ p_1 & p_2 & p_3 \end{bmatrix} \begin{bmatrix} f_1 \\ f_2 \\ f_3 \end{bmatrix} = \underline{0} \quad (5)$$

Nontrivial solutions for f_i requires that

$$\begin{vmatrix} s_{1x} & s_{2x} & s_{3x} \\ s_{1y} & s_{2y} & s_{3y} \\ p_1 & p_2 & p_3 \end{vmatrix} = 0 \quad (6)$$

This situation occurs when the forces are concurrent or parallel. For the configuration of the current device it is not possible for the forces to be parallel and therefore they must meet in a point. This fact is essential for the following derivations.

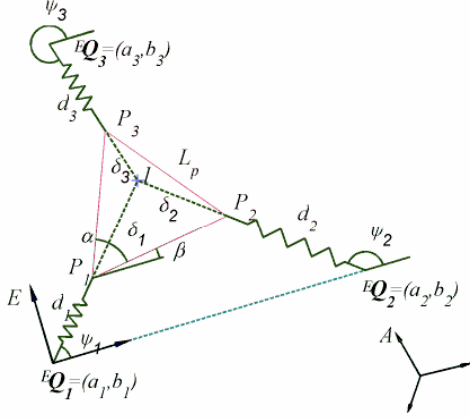


Fig. 4. Nomenclature for the Forward Analysis.

There are several ways to solve the forward analysis problem. Fig. 4 depicts a scheme that shows the variables and parameters used for this model. The elements presented in Fig. 4 have the following meaning:

- Coordinate system A : global reference system
- Coordinate system E : local reference system such that its origin is at point Q_1 , the ${}^E \underline{x}$ axis passes through point Q_2 and the ${}^E \underline{z}$ axis is perpendicular to the plane of the platform
- I : point of intersection of the line of action of the forces acting on the platform
- P_i : point that define the moving platform
- Q_i : free end of the actuator i
- a_i, b_i : coordinates of point Q_i in the local system E
- d_i : current length of the spring i
- δ_i : distance between point P_i and the intersection point I
- ψ_i : angle between d_i and the local x-axis
- β : angle of rotation of the platform with respect to the local x-axis
- L_p : length of a side of the equilateral platform
- α : internal angle of the moving platform and therefore equal to $\pi/3$

Global system A may be located in any arbitrary position. The coordinates of points Q_1, Q_2 , and Q_3 are given in this system. With the knowledge of points Q_i , the local system E is defined as follows

$${}^A \underline{x}_E = \frac{{}^A \underline{Q}_2 - {}^A \underline{Q}_1}{{}^A \underline{Q}_2 - {}^A \underline{Q}_1}} \quad (7)$$

$${}^A \underline{z}_E = \frac{\left({}^A \underline{Q}_2 - {}^A \underline{Q}_1 \right) \times \left({}^A \underline{Q}_3 - {}^A \underline{Q}_1 \right)}{\left| \left({}^A \underline{Q}_2 - {}^A \underline{Q}_1 \right) \times \left({}^A \underline{Q}_3 - {}^A \underline{Q}_1 \right) \right|}} \quad (8)$$

$${}^A \underline{y}_E = {}^A \underline{z}_E \times {}^A \underline{x}_E \quad (9)$$

The transformation that relates systems A and E is given by Crane³ as

$${}^A T_E = \begin{bmatrix} {}^A R & {}^A \underline{Q}_1 \\ 0 & 0 & 0 & 1 \end{bmatrix} \quad (10)$$

where

$${}^A R = \begin{bmatrix} {}^A \underline{x}_E & {}^A \underline{y}_E & {}^A \underline{z}_E \end{bmatrix} \quad (11)$$

The homogeneous coordinates of points Q_i in the system E are given by $[a_i, b_i, 0, 1]^T$ and they can be found from the relation

$${}^E \underline{Q}_i = {}^E T_A {}^A \underline{Q}_i \quad (12)$$

where ${}^E T_A = \left({}^A T_E \right)^{-1}$.

Note that ${}^E \underline{Q}_1$ is the origin of system E and since Q_2 is located on the ${}^E \underline{x}$ axis then

$$a_1 = 0, \quad b_1 = 0, \quad b_2 = 0. \quad (13)$$

Fig. 4 involves ten unknowns, i.e. $d_1, d_2, d_3, \delta_1, \delta_2, \delta_3, \psi_1, \psi_2, \psi_3$, and β . Equations to model the system are obtained from the equilibrium of forces and kinematics considerations.

From Equation 2 and Fig. 4 the equilibrium of forces evaluated in system E yields

$$\begin{aligned} (d_1 - d_0) \begin{bmatrix} \cos \psi_1 \\ \sin \psi_1 \end{bmatrix} + (d_2 - d_0) \begin{bmatrix} \cos \psi_2 \\ \sin \psi_2 \end{bmatrix} \\ + (d_3 - d_0) \begin{bmatrix} \cos \psi_3 \\ \sin \psi_3 \end{bmatrix} = \underline{0} \end{aligned} \quad (14)$$

Since the forces are concurrent, equilibrium of moments does not give any new information. Further equations must be developed based on the kinematics of the device expressed in the system E . From Fig. 4 it is clear that

$$\delta_1 e^{i\psi_1} = L_p e^{i\beta} + \delta_2 e^{i\psi_2} \quad (15)$$

$$\delta_1 e^{i\psi_1} = L_p e^{i(\beta+\alpha)} + \delta_3 e^{i\psi_3}. \quad (16)$$

Loops defined by Q_1 - Q_2 - I and Q_1 - Q_3 - I yield

$$(d_1 + \delta_1) e^{i\psi_1} = {}^E \underline{Q}_2 - {}^E \underline{Q}_1 + (d_2 + \delta_2) e^{i\psi_2} \quad (17)$$

$$(d_1 + \delta_1) e^{i\psi_1} = {}^E \underline{Q}_3 - {}^E \underline{Q}_1 + (d_3 + \delta_3) e^{i\psi_3}. \quad (18)$$

Considering Equation 12, the last two equations can be simplified to

$$(d_1 + \delta_1)e^{i\psi_1} = \begin{bmatrix} a_2 \\ 0 \end{bmatrix} + (d_2 + \delta_2)e^{i\psi_2} \quad (19)$$

$$(d_1 + \delta_1)e^{i\psi_1} = \begin{bmatrix} a_3 \\ b_3 \end{bmatrix} + (d_3 + \delta_3)e^{i\psi_3}. \quad (20)$$

The scalar components of Equations 14, 15, 16, 19, and 20 form a nonlinear system that can be solved using numerical methods. A program to solve the mathematical model for the forward analysis was implemented. The program takes advantage of a function that implements the Newton-Raphson method. Once the variables are found, points ${}^A\underline{P}_i$ are evaluated using the transformation

$${}^A\underline{P}_i = {}^A\underline{T} \quad {}^E\underline{P}_i \quad (21)$$

where points ${}^E\underline{P}_i$ are given by (see Fig. 4)

$${}^E\underline{P}_1 = {}^E\underline{Q}_1 + d_1 \begin{bmatrix} \cos \psi_1 \\ \sin \psi_1 \end{bmatrix} \quad (22)$$

$${}^E\underline{P}_2 = {}^E\underline{P}_1 + L_p \begin{bmatrix} \cos \beta \\ \sin \beta \end{bmatrix} \quad (23)$$

$${}^E\underline{P}_3 = {}^E\underline{P}_1 + L_p \begin{bmatrix} \cos(\beta + \alpha) \\ \sin(\beta + \alpha) \end{bmatrix}. \quad (24)$$

One way to verify the validity of the results is to check if they satisfy equilibrium equations and if the lines of action of the forces intersect at the same point, when they are evaluated in the global system A, instead of the local system E.

The equilibrium condition in the global system can be written as

$$\Sigma \underline{F} = k(d_1 - d_0)\underline{s}_1 + k(d_2 - d_0)\underline{s}_2 + k(d_3 - d_0)\underline{s}_3 \quad (23)$$

where

$$\underline{s}_i = \frac{{}^A\underline{Q}_i - {}^A\underline{P}_i}{{}^A\underline{Q}_i - {}^A\underline{P}_i} \quad (24)$$

The intersection point of the lines passing through points P_1-Q_1 and P_2-Q_1 and P_2-Q_2 is given by (Crane, C., Rico, J., Duffy, J., Screw Theory for Spatial Robot Manipulators, Cambridge University Press, In Preparation)

$${}^A\underline{r}_{12} = \frac{\underline{s}_2 \times \underline{s}_{02} - (\underline{s}_1 \cdot \underline{s}_2)\underline{s}_1 \times \underline{s}_{02} + (\underline{s}_1 \times \underline{s}_{01} \cdot \underline{s}_2)\underline{s}_2}{1 - (\underline{s}_1 \cdot \underline{s}_2)^2} \quad (25)$$

Similarly, the intersection of lines passing through P_2-Q_2 and P_3-Q_3 is given by

$${}^A\underline{r}_{23} = \frac{\underline{s}_3 \times \underline{s}_{03} - (\underline{s}_2 \cdot \underline{s}_3)\underline{s}_2 \times \underline{s}_{03} + (\underline{s}_2 \times \underline{s}_{02} \cdot \underline{s}_3)\underline{s}_3}{1 - (\underline{s}_2 \cdot \underline{s}_3)^2} \quad (25)$$

where

$$\underline{s}_{0i} = {}^A\underline{Q}_i \times \underline{s}_i. \quad (26)$$

Lines of action of external forces intersect if ${}^A\underline{r}_{12} = {}^A\underline{r}_{23}$. Numerical cases have been analyzed and they have shown that the points ${}^A\underline{r}_{12}$ and ${}^A\underline{r}_{23}$ are coincident for the cases that were considered.

IV. RESULTS

This paper has presented an overview of the design of a spatial compliant microplatform. The device has three degrees of freedom as represented by the three bimetallic actuators. A feature of the device is that it can be manufactured in the plane and then deployed spatially to a desired orientation.

A forward analysis of the device has been presented. In this analysis, the position and orientation of the platform is determined based on knowledge of the three input actuator lengths. A numerical solution technique was employed due to the complexity of the analysis whereby it was necessary to determine ten parameters that would simultaneously satisfy a set of constraint equations.

ACKNOWLEDGEMENTS

The authors would like to gratefully acknowledge the support of the Department of Energy, grant number DE-FG04-86NE37967. This work was accomplished as part of the DOE University Research Program in Robotics (URPR).

REFERENCES

1. Chen, W., Chien, C. Hsieh, J., and Fang, W., 2003, "A Reliable Single-Layer Out-of-Plane Micro-machined Thermal Actuator," Sensors and Actuators A, 103(1-2), pp. 48-58.
2. Fu Y., Du H., Huang W., and Hu, M., 2004, "TiNi-Based Thin Films in MEMS Applications: a Review," Sensors and Actuators A, 112(2-3), pp. 395-408.
3. Jain, A., Xie, H., "A single-Crystal Silicon Micromirror for Large Bi-Directional 2D scanning applications," Sensors and Actuators A, Article in Press.
4. Ebefors, T., Mattsson, J., Kalvesten, E. and Stemme, G., 1999, "A Robust Micro Conveyor Realized By

- Arrayed Polyimide Joint Actuators,” IEEE Paper No 0-7803-5194-0/99.
5. Suh, J., Darling, R., Bohringer, K., Donald, B., Baltes, H., and Kovacs, G., 1999, “CMOS Integrated Ciliary Actuator Array as a General-Purpose Micro-manipulation Tool for Small Objects,” *Journal of Microelectromechanical Systems*, 8(4), pp. 483-496.
 6. Schweizer, S., Calmes, S., Laudon, M., and Renaud, P., 1999, “Thermally Actuated Optical Microscanner with Large Angle and Low Consumption,” *Sensors and Actuators A*, 76(1-3), pp. 470-477.
 7. Jensen K., Howell L., and Lusk K. 2004, “Force Relationships for an XYZ Micromanipulator with Three Translational Degrees of Freedom,” *Proceedings Design Engineering Technical Conferences, ASME, Salt Lake City, Utah, USA.*
 8. Bamberger, H. and Shoham, M., 2004, “Kinematic Structure of a Parallel Robot for MEMS Fabrication,” *Proceedings On Advances in Robot Kinematics, Netherlands*, pp. 113-122.
 9. Fuller, R., 1975, *Synergetics, Explorations in the Geometry of Thinking*, Collier Macmillan, London.
 10. Kenner, H., 1976, *Geodesic Math and How to Use It*, University of California Press, Berkeley.
 11. Calladine, C., 1978, “Buckminster Fuller’s Tensegrity Structures and Clerk Maxwell’s Rules for the Construction of Stiff Frames,” *International Journal of Solids and Structures*, 14, pp. 161-172.
 12. Murakami, H., 2001, “Static and Dynamic Analyses of Tensegrity Structures. Part 1. Nonlinear Equations of Motion,” *International Journal of Solids and Structures*, 38, pp. 3599-3613.
 13. Crane, C., Duffy, J. and Correa, J., 2005, “Static Analysis of Tensegrity Structures,” *Journal of Mechanical Design*, 127(2), pp. 257-268.
 14. Knight, B.F., 2000, “Deployable Antenna Kinematics using Tensegrity Structure Design,” Ph.D. thesis, University of Florida, Gainesville, FL.
 15. Sultan, C., and Corless, M., 2000, “Tensegrity Flight Simulator,” *Journal of Guidance, Control, and Dynamics*, 23(6), pp. 1055-1064.
 16. Tibert, A., and Pellegrino S., 2002, “Deployable Tensegrity Reflectors for Small Satellites,” *Journal of Spacecraft and Rockets*, 39(5), pp.701-709.
 17. Sultan, C., and Skelton, R., 2004, “A Force and Torque Tensegrity Sensor,” *Sensors and Actuators A*, 112(2-3), pp. 220-231.
 18. Ingber, D. E., 1993, “Cellular Tensegrity: Defining New Rules of Biological Design That Govern the Cytoskeleton,” *J. Cell. Sci.*, 104, pp. 613-627.